The ATLAS detector performance

Rosy NICOLAIDOU[*][†]

CEA-Saclay, DSM/IRFU/SPP
91191 Gif sur Yvette, France
E-mail: Rosy.Nicolaidou@cern.ch

The status and performance of the ATLAS detector with the data taken in 2010 from proton-proton (pp) collisions at the centre-of-mass energy of 7 TeV delivered by the Large Hadron Collider at CERN as well as from the heavy ion lead-lead collisions at centre-of-mass energy of 2.76 TeV, are presented in this paper. Highlights from physics results from pp collisions reviewed here include studies on physics with jets, *W* and *Z* bosons as well as top quark pair production. Highlights from results from the heavy ion collision run are also reviewed.

---

[*]Speaker.
[†]On behalf of the ATLAS Collaboration

1. The ATLAS detector

The ATLAS detector [1] covers almost the whole solid angle around the collision point with layers of tracking detectors, calorimeters and muon chambers. The Inner-Detector (ID) system is immersed in a 2 T axial field and provides tracking, vertexing and $e - \pi$ separation in the pseudo-rapidity range of $|\eta| \leq 2.5$. It consists of pixel and silicon microstrip detectors surrounded by a Transition Radiation Tracker (TRT). The calorimeter system covers the pseudorapidity range $|\eta| <$ 4.9 and uses a variety of techniques. The electromagnetic calorimeter is a liquid argon (LAr) detector using lead as the absorber in the barrel region and copper in the forward region; it provides $e - \gamma$ trigger, identification and measurement. The hadronic calorimeter with scintillator tiles or LAr as the active material and with either steel, copper or tungsten as the absorber material, provides trigger, jet measurements and missing transverse energy measurement. Finally the Muon Spectrometer is based on the magnetic deflection of muon tracks in the large superconducting air-core toroid magnets, instrumented with separate trigger and high-precision tracking chambers covering the pseudorapidity range up to $|\eta| <$2.7.

The trigger system of ATLAS comprises three levels: the first of which (L1) is fully hardware, implemented in the calorimeters and the Muon Spectrometer. The other two levels, the level two (L2) and the Event Filter (EF) are software based: the L2 accepts data from defined Regions Of Interests (ROI) of L1 and the EF provides a full event reconstruction on computer farms.

A schematic view of the ATLAS detector is shown in Figure 1.

1.1 Luminosity and Detector Status

From March to November 2010 the LHC delivered pp collisions at centre-of-mass energy of 7 TeV. The instantaneous luminosity increased during this period almost five orders of magnitude, from $\mathscr{L} \approx 10^{27}$ cm $^{-2}$s^{-1} to $\mathscr{L} \approx 2.1 \times 10^{32}$ cm $^{-2}$s^{-1}. The total integrated luminosity was 48 pb^{-1} out of which 45 pb^{-1} were recorded by ATLAS leading to an overall data taking efficiency of 94%. At the end of November 2010 the LHC delivered 9.7 μb^{-1} of PbPb collisions at centre-of-mass energy of nucleon pairs of 2.76 TeV and $\approx$9.1 μb^{-1} were recorded by ATLAS. All the sub-detectors of ATLAS operated with a very high efficiency > 97%.

The LHC luminosity has been measured in ATLAS using diferent detectors and methods[2]. The absolute luminosity calibration was obtained using the van der Meer beam separation scans method[3] with a systematic uncertainty of 3.4%[4].

1.2 Inner Detector Performance

The tracking performance of the Inner Detector was assessed via the observation of well measured particle decays, like K_s^0, ϕ, D mesons and Ω, Ξ, Λ baryons. Clear signals of all these resonances were obtained in data. Figure 2 shows two examples of such particles namely the reconstruction of K_s^0 decaying to a pair of pions and the J/ψ decaying to a pair of muons. Those studies allowed the momentum scale to be determined at the per mill level for the low transverse momentum (P$_T$) region, and for higher momentum at the % level (for momentum up to 100 GeV). The resolution was found as expected to be dominated by multiple scattering in the low P$_T$ region.
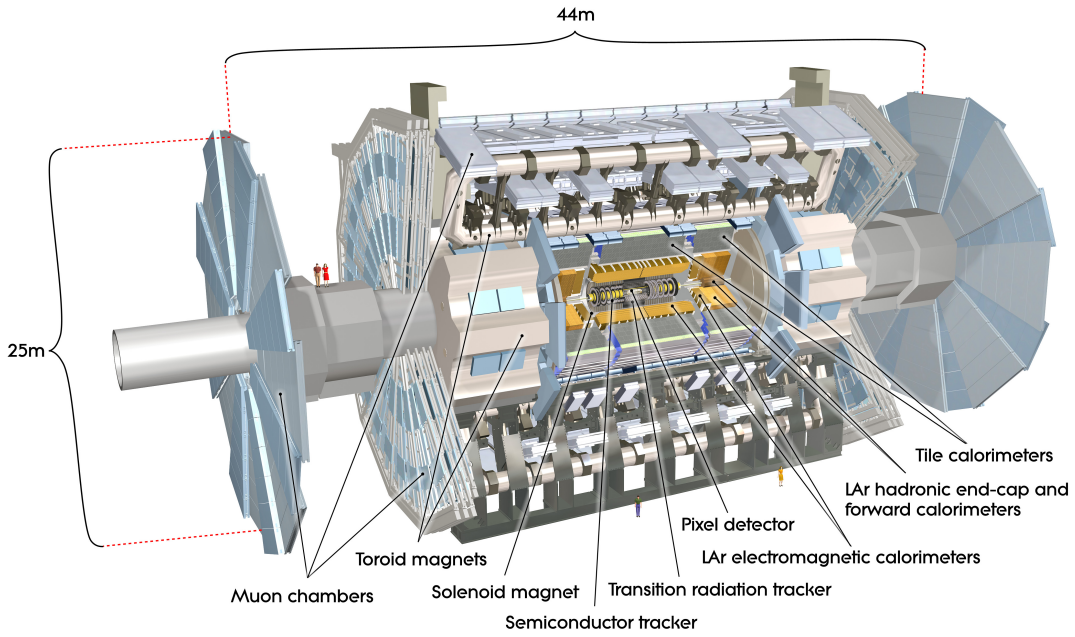
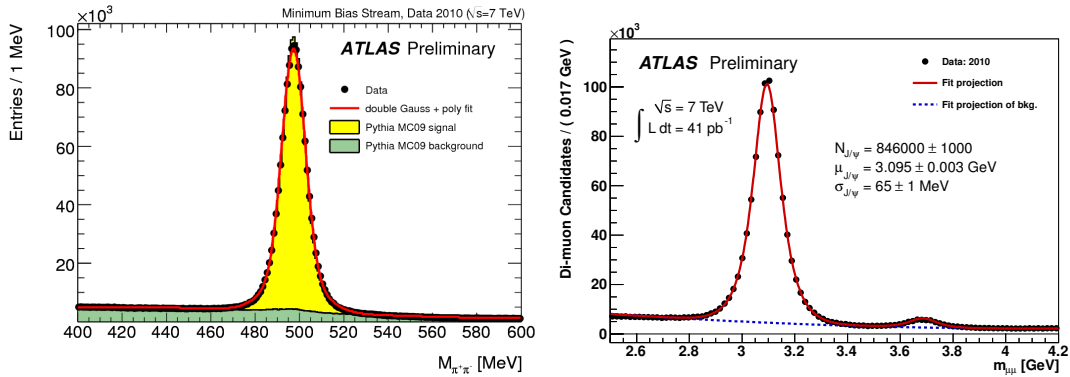**Figure 1:** Schematic view of the ATLAS detector.

Figure 2: Left plot: Reconstruction of K^0_s invariant mass in the barrel region (both tracks are in $|\eta| < 1.2$). The black circles are the data, while the histograms show the Monte Carlo simulation (normalized to the data). The red line is the line-shape function fitted to data [5]. Right plot: Di-muon invariant mass spectrum at the J/ψ and $\psi(2S)$ mass range.

1.3 Calorimeter Performance

Performance of the electromagnetic (em) calorimeter: The initial validation of the energy deposits in the calorimeter of the em showers, was done from test-beam measurements in the past. With the first data of 2009 at $\sqrt{s} = 900$ GeV the signal of a π^0 decaying to a pair of photons was extracted [6] as can be seen on the left plot of Figure 3. From the comparison of its mass to the Particle Data Group (PDG) value the energy scale was checked within 2%. The em scale has been determined on 7 TeV centre-of-mass-energy data using the *Z* boson decays to a pair of
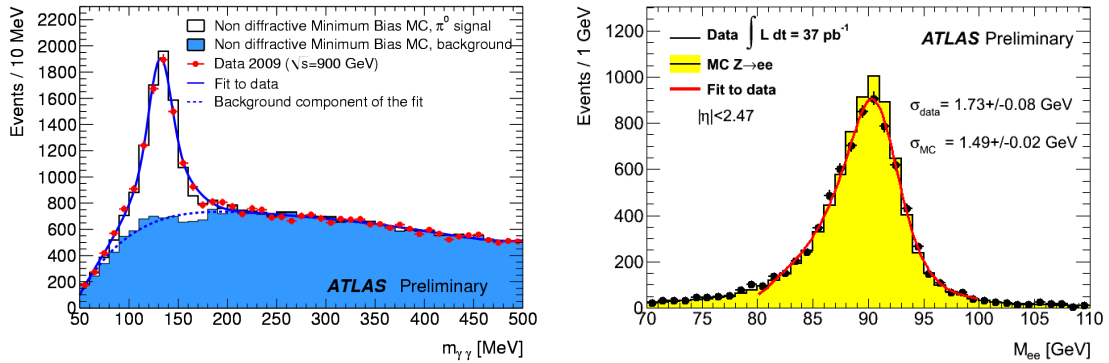
Figure 3: Left plot: Diphoton invariant mass in the region around the π^0 mass. A fit is superimposed to the red points that represent the data; the histogram represents the Monte Carlo prediction normalized to the data entries. Right plot: The invariant mass distribution of e^+e^- candidates in the Z boson mass region. Black points represent tha data and the histogram the Monte Carlo prediction.

electrons. Events with two opposite charge electrons reconstructed with transverse energy $E_T >$ 20 GeV and constraint their mass to follow the well known Z line shape derived from simulation. This method was applied in different em regions. The right plot of Figure 3 shows the distribution of this calibrated Z mass, after applying the corrections to the electron energy.

Performance of the hadronic calorimeter: Understanding and measuring the performance of jets is crucial for many physics analyses at the LHC. The uncertainty of the jet energy calibration is the dominant experimental uncertainty for numerous physics results with jets and has been evaluated on data for jets with transverse momenta above 20 GeV up to the kinematic limit of 3.5 TeV and $|\eta|$ up to 4.5. Jets were reconstructed with the anti-kt [7] algorithm with distance parameters of 0.6 and 0.4. The left plot of Figure 4 shows the final fractional jet energy scale systematic uncertainty as a function of p_T^{jet} for the barrel region. For example it is found to be less that 2.5% in the region of jet transverse momenta between 60 and 800 GeV.

The calorimeters allow also for the measurement of the missing transverse energy E_T^{miss}, a quantity sensitive to the calorimeter performance in terms of noise dead cells and miscalibration as well as for beam backgrounds and cosmics. It has been measured in the ATLAS detector with the 7 TeV collision data [9] and found to be in reasonable agreement with the simulation (right plot of Figure 4).

1.4 Muon Spectrometer Performance

The performance of the MS is also assessed via the reconstruction of well known particle decays. Figure 5 shows the invariant mass of two opposite charge muons of $p_T > 15$ GeV that are coming from a common vertex. The J/ψ and Z resonances are used to study in detail the performance of the MS in the low and high p_T regime respectively. The muon reconstruction efficiency as measured on data with "tag and probe" techniques [10], [11] was found to be consistent with the simulation predictions; for example the average efficiency for muons of $p_T > 5$ GeV is $\approx 98\%$. The J/ψ decays gave a unique opportunity to probe the efficiency measurement down to very low values of p_T. The K_s^0 decays to a pair of pions were used to study the muon fake rate (i.e
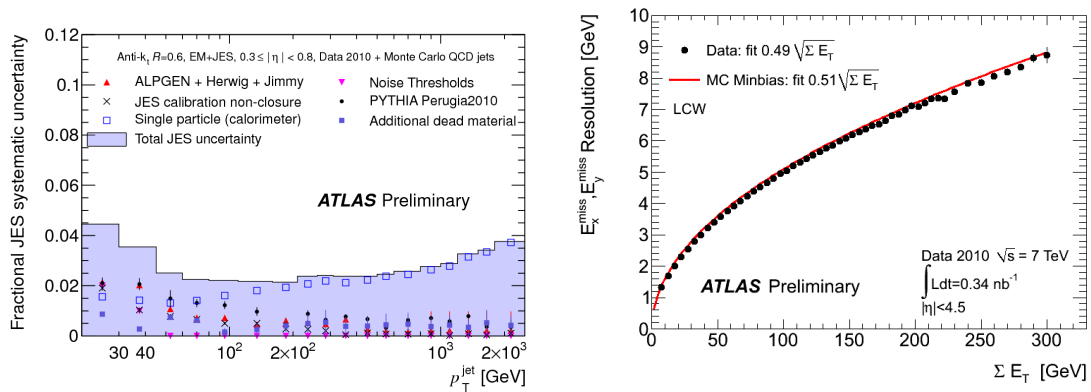
Figure 4: Left plot: Fractional jet energy scale systematic uncertainty as a function of p_T^{jet} for jets in the pseudorapidity range $0. < |\eta| < 0.8$ in the barrel calorimeter. The total uncertainty is shown as the solid light blue area [8]. Right plot: Resolution of the transverse missing energy (E_x^{miss}, E_y^{miss}) as a function of the total transverse energy ΣE_T for pp collision data at centre of mass energy of 7 TeV. Full dots represent the data while the line is a fit to the resolution obtained in Monte Carlo simulations.
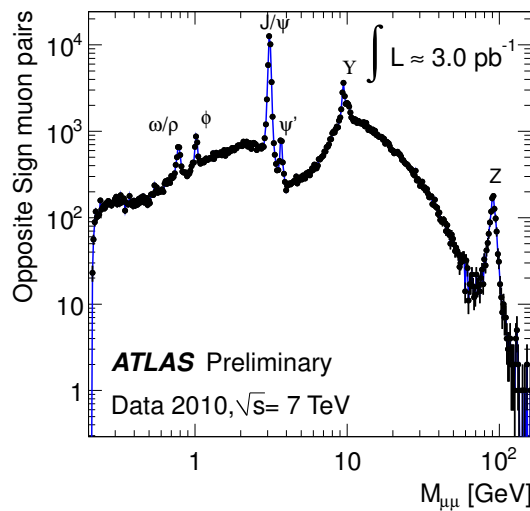

Figure 5: Dimuon invariant mass spectrum of two opposite charge muons of $p_T > 15$ GeV that are coming from a common vertex.

the muon background from decays in flight or reconstruction ghosts) which was found to be of the order of 1 per mill [12].

2. Highlights from physics results

2.1 Results from pp collisions

2.1.1 Physics with Jets

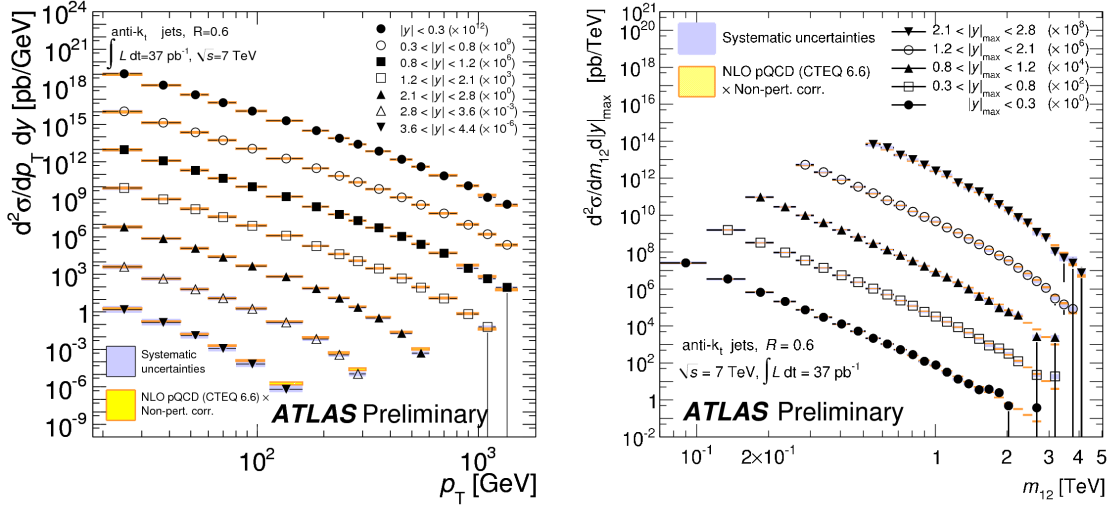Jet cross sections serve as one of the main observables in high-energy particle physics, and

Figure 6: Left plot: The double-differential inclusive jet cross section is shown for jets reconstructed with the anti-kt algorithm with R = 0.6 as a function of the p_T of the jet for 7 rapidity bins. Right plot: The dijet double-differential cross section as a function of dijet mass, binned in the maximum rapidity of the two leading jets. In both plots, for convenience, the cross sections are multiplied by the factors indicated in the legend and the data are compared to Next to Leading Order (NLO) perturbative QCD (pQCD) calculations to which non-perturbative corrections have been applied. More details can be found on [13].

constitute one of the first measurements performed after the startup of new colliders. Jet measurements have provided precise measurements of the strong coupling constant, and are an important tool for understanding the strong interaction and searching for physics beyond the Standard Model. ATLAS has measured the inclusive singe-jet and dijet double-differential cross section as a function of the tranverse momentum of the jet p_T in different regions of rapidity $|y|$ [13]. The left plot of Figure 6 shows the inclusive jet double-differential cross section as a function of jet p_T for seven rapidity bins. The measurement extends from jet transverse momentum of 20 GeV to almost 1.5 TeV, spanning two orders of magnitude in p_T and seven orders of magnitude in cross section. On the right plot of Figure 6 the dijet double-differential cross section as a function of dijet mass, binned in the maximum rapidity of the two leading jets, is shown.

The 37.3 pb[1] data of 2010 sample led to inclusive jet measurements up to 1.4 TeV, and dijet mass measurements up to 4.1 TeV. These measurements, probed next-to-leading order (NLO) pQCD and parton distribution functions (PDFs) in a new kinematic regime.

2.1.2 W, Z **boson physics**

The leptonic decays of W, Z bosons are used to calibrate the detector, while they constitute the main backgrounds to new physics processes. Around 260 thousand W and 26 thousand Z leptonic decays were recorded by ATLAS in 2010 data taking. Two examples of this type of physics are described in this section. ATLAS has measured the total $W^{\pm} \to l^{\pm}\nu$ and $Z/\gamma^* \to l^+l^-$, $l = e, \mu$ cross section as well as their ratios [14]. The left plot of Figure 7 shows the measured
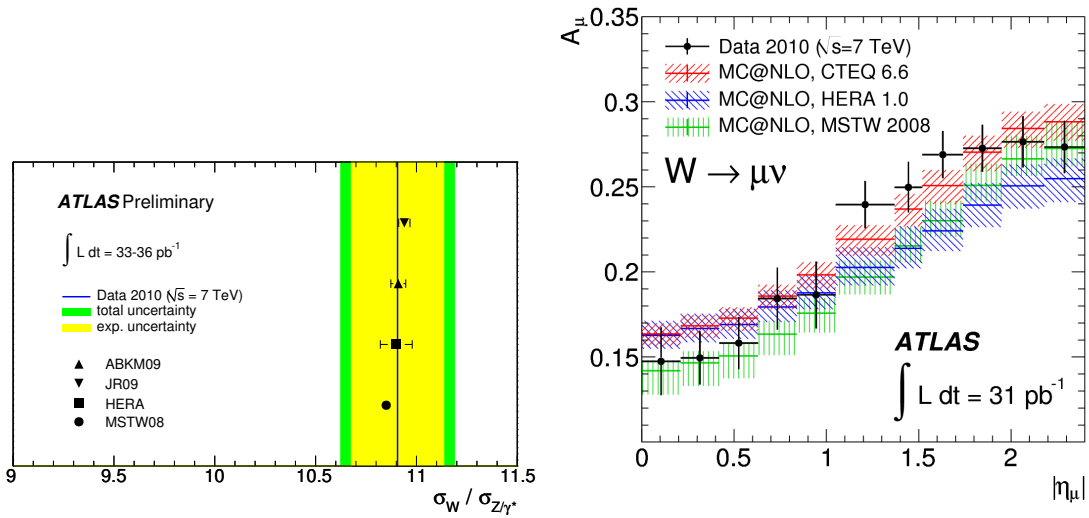
6

Figure 7: Left plot: Measured and predicted W/Z cross section ratio. The experimental uncertainty of the measurement includes statistical and experimental systematic errors. Right plot: Muon charge asymmetry from $W^\pm \to \mu^\pm \nu$ decays in bins of absolute pseudorapidity [15]. The kinematic requirements applied are $p_{\mu_T} > 20$ GeV, $p_{\nu_T} > 25$ GeV and $m_T > 40$ GeV. The data points (shown with error bars including the statistical and systematic uncertainties) are compared to MC@NLO predictions with different PDF sets.

cross section ratio $(\sigma_{W^+} + \sigma_{W^-})/\sigma_{Z/\gamma^*}$ as a vertical band compared with the theoretical predictions. These predictions agree very well with the measurement.

Another example is the measurement of the charge asymmetry of leptons originating from the decay of singly produced W bosons that was performed with the ATLAS pp collision data and provides important information about the proton structure as described by the PDFs. The W boson charge asymmetry is mainly sensitive to valence quark distributions via the dominant production process $u\bar{d}(\bar{u}d) \to W^{+(-)}$. The right plot of the Figure 7 shows the muon charge asymmetry from W boson decays to a muon and a neutrino in bins of absolute pseudorapidity [15]. With the LHC data it became kinematically possible to precisely measure the valence quark distributions and in particular the ratio of u/d quarks below the parton momentum fraction range of $x < 0.05$. The input of this analysis is expected to contribute to the determination of the next generation of PDF sets, helping to reduce the PDF uncertainties, particularly the shapes of the valence quark distributions in the low-x region.

2.1.3 Production of top quarks $t\bar{t}$

The measurement of the top-quark pair-production cross-section $\sigma_{t\bar{t}}$ is one of the milestones for the early LHC physics program. A precise measurement of $\sigma_{t\bar{t}}$ allows precision tests of perturbative QCD, where uncertainties on $\sigma_{t\bar{t}}$ are now at the level of 10% [1]. In addition $t\bar{t}$ production is an important background to the search for the Higgs boson and various searches for physics beyond the Standard Model.

ATLAS has measured the production cross section of $t\bar{t}$ [16] combining the results of two channels, the single lepton channel (with one lepton (e,μ), large missing transverse energy and
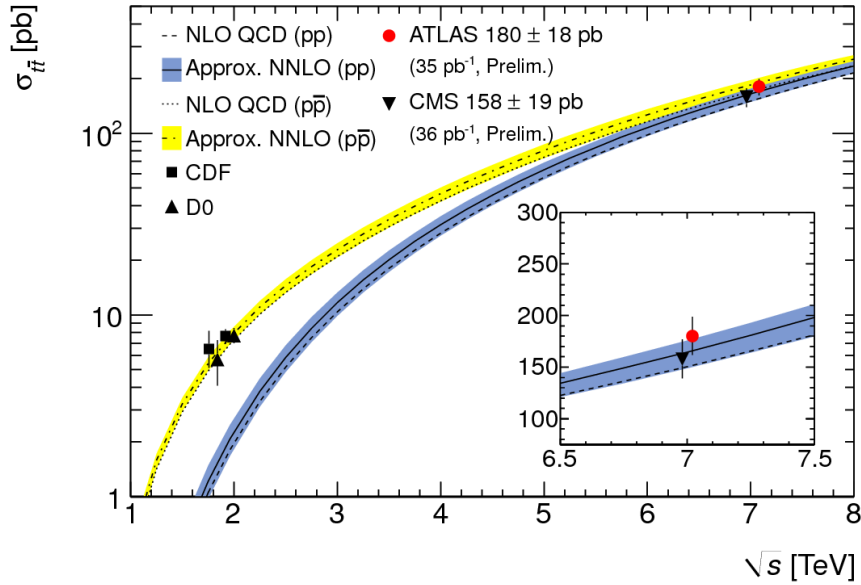
Figure 8: Measurements of $\sigma_{t\bar{t}}$ from ATLAS and CMS in pp collisions, and CDF and D0 in p$\bar{p}$ collisions compared to theoretical predictions assuming a top mass of 172.5 GeV as a function of $\sqrt{s}$. The ATLAS result is indicated by the red circle.

at least four jets) and the dilepton channel (two leptons (ee, $\mu\mu$ or eμ), large missing transverse energy and at least two jets). The result is $\sigma_{t\bar{t}} = 189 \pm 9$ (stat.) ± 15 (syst.) ± 6 (luminosity) pb, which is in excellent agreement with the Standard Model prediction. Figure 8 shows various cross-section measurements from Tevatron and LHC results overlaid with the theoretical predictions as a function of centre-of-mass energy.

2.2 Results from heavy ion PbPb collisions

At the end of 2010, the LHC delivered a short run of PbPb collisions at centre-of-mass energy of nucleons at 2.76 TeV. Heavy ion collisions at these ultrarelativistic energies can probe quark gluon plasma physics. An interesting observation, the so called 'jet quenching', which is the production of highly unbalnaced jets with one jet produced at the periphery of the collision, gives hints of how the parton shower develops in this dense medium. The jet quenching is expected in central heavy ion collisions and actually at Relativistic Heavy Ion Collider experiments (RHIC) quenching in two particle correlation is observed.

With the data collected by the ATLAS detector observations have been made of a centrality-dependent dijet asymmetry in these collisions [17]. Events with two jets were selected requiring the leading jet to have transverse energy $E_T > 100$ GeV and the second jet $E_T > 25$ GeV. The transverse energies of dijets in opposite hemispheres were observed to become systematically more unbalanced with increasing event centrality leading to a large number of events which contain highly asymmetric dijets as it is shown in Figure 9.

This was the first observation of an enhancement of events with such large dijet asymmetries, not observed in proton-proton collisions, which may point to an interpretation in terms of strong
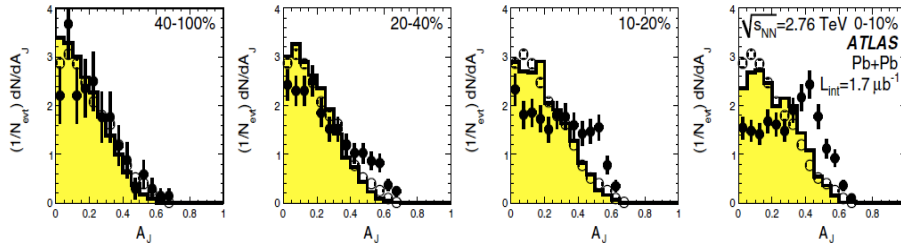
Figure 9: Dijet asymmetry distributions for data (points) and unquenched HIJING with superimposed PYTHIA dijets (solid yellow histograms), as a function of collision centrality (left to right from peripheral to central events). Proton-proton data from $\sqrt{s} = 7$ TeV analyzed with the same jet selection, are shown as open circles.

jet energy loss in a hot, dense medium.

3. Summary and Conclusions

The ATLAS collaboration has delivered a plethora of physics results with the 2010 data. The ATLAS detector performed very well throughout this period. The Standard Model processes were "rediscovered" up to the production of top quarks. Many searches already extended the limits set by previous colliders. The first observation of dijet asymmetries in heavy ion collisions were made. All these achievements were possible thanks to the fantastic LHC machine team and to the many years of dedicated work in commissioning of the ATLAS detector.

References

[1] ATLAS Collaboration, G. Aad et al., *The ATLAS Experiment at the CERN Large Hadron Collider*, JINST **3** (2008) S08003.

[2] ATLAS Collaboration, G. Aad et al., *Luminosity Determination Using the ATLAS Detector*, ATLAS-CONF-2010-060.

[3] S. van der Meer, *Calibration of the effective beam height in the ISR*, CERN-ISR-PO-68-31, 1968.

[4] ATLAS Collaboration, G. Aad et al., *Updated Luminosity Determination in pp Collisions at $\sqrt{s} = 7$ TeV using the ATLAS detector*, ATLAS-CONF-2011-011.

[5] ATLAS Collaboration, G. Aad et al., *Kinematic Distributions of K_s^0 and Λ^0 decays in collision data at $\sqrt{s} = 7$ TeV*, ATLAS-CONF-2010-033.

[6] ATLAS Collaboration, G. Aad et al., *Performance of the ATLAS electromagnetic calorimeter for $\pi^0 \to \gamma\gamma$ and $\eta \to \gamma\gamma$ events*, ATLAS-CONF-2010-006.

[7] M. Cacciari, G. P. Salam and G. Soyez, *The anti-kt jet clustering algorithm*, JHEP 04 (2008) 063.

[8] ATLAS Collaboration, G. Aad et al., *Jet energy scale and its systematic uncertainty in proton-proton collision at $\sqrt{s} = 7$ TeV with ATLAS 2010 data*, ATLAS-CONF-2011-032.

[9] ATLAS Collaboration, G. Aad et al., *Performance of the Missing transverse Energy Reconstruciton and Calibration in Proton-Proton Collisions at a Centre-of-Mass Energy of $\sqrt{s} = 7$ TeV with the ATLAS Detector*, ATLAS-CONF-2010-057.

[10] ATLAS Collaboration, G. Aad et al., *A measurement of the ATLAS muon reconstruction and trigger efficiency using J/ψ decays*, ATLAS-CONF-2011-021.

[11] ATLAS Collaboration, G. Aad et al., *Determination of the muon reconstruction efficiency in ATLAS at the Z resonance in proton-proton collisions at $\sqrt{s}$=7 TeV*, ATLAS-CONF-2011-008.

[12] ATLAS Collaboration, G. Aad et al., *Muon reconstruction Performance*, ATLAS-CONF-2010-064.

[13] ATLAS Collaboration, G. Aad et al., *Measurement of inclusive jet and dijet cross sections in proton-proton Collision data at 7 TeV centre-of-mass Energy using the ATLAS Detector*, ATLAS-CONF-2011-047.

[14] ATLAS Collaboration, G. Aad et al., *A measurement of the total $W^{\pm}$ ans $Z\gamma^*$ cross sections in the e,μ decay channels and of their ratios in pp collisions at $\sqrt{s} = 7$ TeV with the ATLAS Detector*, ATLAS-CONF-2011-041.

[15] ATLAS Collaboration, G. Aad et al., *Measurement of the Muon Charge Asymmetry from W Bosons Produced in pp Collisions at $\sqrt{s} = 7$ TeV with the ATLAS Detector*, submitted to Phys. Lett. B, arXiv:1103.2929v1.

[16] ATLAS Collaboration, G. Aad et al., *A combined measurement of the top quark pair production cross-section using dilepton and single-lepton final states*, ATLAS-CONF-2011-040.

[17] ATLAS Collaboration, G. Aad et al., *Observation of a Centrality-Dependent Dijet Asymmetry in Lead-Lead Collisions at $\sqrt{s_{NN}} = 2.76$ TeV with the ATLAS Detector at the LHC*, Phys. Rev. Lett. 105,252303 (2010).